Wired and wireless convergent extended-reach optical access network using direct-detection of all-optical OFDM super-channel signal

C. W. Chow,[1,*] C. H. Yeh,[2] J. Y. Sung,[1] and C. W. Hsu[1]

[1]*Department of Photonics and Institute of Electro-Optical Engineering, National Chiao Tung University, Hsinchu 30010, Taiwan*
[2] *Department of Photonics, Feng Chia University, Seatwen, Taichung 40724, Taiwan*
*cwchow@faculty.nctu.edu.tw

Abstract: We propose and demonstrate the feasibility of using all-optical orthogonal frequency division multiplexing (AO-OFDM) for the convergent optical wired and wireless access networks. AO-OFDM relies on all-optically generated orthogonal subcarriers; hence, high data rate (> 100 Gb/s) can be easily achieved without hitting the speed limit of electronic digital-to-analog and analog-to-digital converters (DAC/ADC). A proof-of-concept convergent access network using AO-OFDM super-channel (SC) is demonstrated supporting 40 – 100 Gb/s wired and gigabit/s 100 GHz millimeter-wave (MMW) ROF transmissions.

References and links

1. Z. Xu, Y. J. Wen, W. D. Zhong, M. Attygalle, X. Cheng, Y. Wang, T. H. Cheng, and C. Lu, "WDM-PON architectures with a single shared interferometric filter for carrier-reuse upstream transmission," J. Lightwave Technol. **25**(12), 3669–3677 (2007).
2. G. K. Chang, A. Chowdhury, Z. Jia, H. C. Chien, M. F. Huang, J. Yu, and G. Ellinas, "Key technologies of WDM-PON for future converged optical broadband access networks," J. Opt. Commun. Netw. **1**(4), C35 (2009).
3. L. Deng, M. Beltrán, X. Pang, X. Zhang, V. Arlunno, Y. Zhao, A. Caballero, A. Dogadaev, X. Yu, R. Llorente, D. Liu, and I. T. Monroy, "Fiber wireless transmission of 8.3-Gb/s/ch QPSK-OFDM signals in 75–110-GHz band," IEEE Photon. Technol. Lett. **24**(5), 383–385 (2012).
4. H. H. Lu, H. C. Peng, W. S. Tsai, C. C. Lin, S. J. Tzeng, and Y. Z. Lin, "Bidirectional hybrid CATV/radio-over-fiber WDM transport system," Opt. Lett. **35**(3), 279–281 (2010).
5. P. C. Peng, H. Y. Wang, C. H. Chang, H. L. Hu, W. Y. Yang, and F. K. Wu, "DSBCS modulation scheme for hybrid wireless and cable television system," Opt. Express **22**(1), 1135–1142 (2014).
6. S. Cherry, "Edholm's law of bandwidth," IEEE Spectr. **41**(7), 58–60 (2004).
7. N. Cvijetic, "OFDM for next-generation optical access networks," J. Lightwave Technol. **30**(4), 384–398 (2012).
8. Y. C. Chi, Y. C. Li, and G. R. Lin, "Specific jacket SMA-connected TO-can package FPLD transmitter with direct modulation bandwidth beyond 6 GHz for 256-QAM single or multisubcarrier OOFDM up to 15 Gb/s," J. Lightwave Technol. **31**(1), 28–35 (2013).
9. C. W. Chow, C. H. Yeh, C. H. Wang, F. Y. Shih, C. L. Pan, and S. Chi, "WDM extended reach passive optical networks using OFDM-QAM," Opt. Express **16**(16), 12096–12101 (2008).
10. W. R. Peng, I. Morita, H. Takahashi, and T. Tsuritani, "Transmission of high-speed (> 100 Gb/s) direct-detection optical OFDM superchannel," J. Lightwave Technol. **30**(12), 2025–2034 (2012).
11. K. Xu, J. Y. Sung, C. Y. Wong, Z. Cheng, C. W. Chow, and H. K. Tsang, "Optical Nyquist filters based on silicon coupled resonator optical waveguides," Opt. Commun. **329**, 23–27 (2014).
12. M. C. Parker, R. Martin, K. Guild, and S. D. Walker, "Hierarchical wireless and optical access networking: convergence and energy efficiency," Proc. ICTON 2011, Tu.D3.5.
13. A. Rahim, S. Schwarz, J. Bruns, C. G. Schäffer, and K. Petermann, "Terabit optical OFDM demultiplexer in silicon photonics," Proc. OFC, 2013, Paper JTh2A.28.
14. W. Jiang, K. Okamoto, F. M. Soares, F. Olsson, S. Lourdudoss, and S. J. B. Yoo, "5 GHz channel spacing InP-based 32-channel arrayed-waveguide grating," Proc. OFC 2009, OWO2.
15. A. D. Ellis and F. C. G. Gunning, "Spectral density enhancement using coherent WDM," IEEE Photon. Technol. Lett. **17**(2), 504–506 (2005).
16. C. W. Chow, C. H. Yeh, and J. Y. Sung, "OFDM RF power-fading circumvention for long-reach WDM-PON," Opt. Express **22**(20), 24392–24397 (2014).

1. Introduction

Broadband wired networks based on passive optical network (PON) access technologies can provide high bandwidth services to users using low loss and low cost optical fibers [1]. However, they are not flexible enough to allow convenient roaming connections. On the other hand, wireless access technologies can provide high flexibility to users; however, they do not have the abundant bandwidth for high-definition and high-quality video transmissions. Hence wired and wireless convergent network architectures have been proposed [2, 3]. This can be achieved by transmitting both baseband and radio frequency (RF) signals simultaneously using radio-over-fiber (ROF) technologies [2–5]. Interestingly, major carriers also have a similar predication (known as Edholm's Law of bandwidth) [6]. It states that the data rate increase of wireless communication will be much faster than that in wired communication. The data rate of both wired and wireless networks will converge at ~2030.

Optical orthogonal frequency division multiplexing (O-OFDM) is a promising candidate for the high-speed optical access networks. In this OFDM-PON, different OFDM subcarriers can be assigned to different optical network units (ONUs). As a result, the network capacity can be aggregated and de-aggregated electronically on an optical carrier [7, 8]. O-OFDM is highly spectral-efficient and highly chromatic-dispersion tolerant; hence it is suitable for long-reach (LR) or extended-reach (ER) PON [9]. Direct-detection (DD) O-OFDM can also be used to lower the cost of the cost-sensitive PON [10]. As the O-OFDM signal is electronically generated and demodulated by inverse fast Fourier transform (IFFT) and FFT using electronic digital-to-analog and analog-to-digital converters (DAC/ADC), the O-OFDM signal bandwidth is significantly limited by the sampling rate of these electric devices.

In this work, we propose and demonstrate the feasibility of using all-optical (AO)-OFDM for the convergent optical wired and wireless access networks. AO-OFDM relies on all-optically generated orthogonal subcarriers; hence, high data rate (> 100 Gb/s) can be easily achieved without hitting the speed limit of electronic DAC/ADC. A proof-of-concept convergent access network using AO-OFDM super-channel (SC) is demonstrated supporting 40 – 100 Gb/s wired and gigabit/s 100 GHz millimeter-wave (MMW) ROF transmissions.

2. Architecture of the proposed AO-OFDM convergent access network

The proposed architecture of AO-OFDM access network is shown in Fig. 1. For the downstream transmission, a continuous-wave (CW) signal is launched into an "Optical Tone Generator (OTG)" to produce multiple coherent optical tones for the AO-OFDM-SC at the optical line terminal (OLT). In our experiment, the OTG is consisted of two cascaded phase modulators (PMs), which are electrically driven at 20 GHz and 5 GHz respectively. Hence, multiple phase-locked optical combs with frequency separation of 5 GHz are produced. Then the optical combs are wavelength de-multiplexed and encoded by 5 Gb/s non-return-to-zero (NRZ) signals using optical intensity modulators (MODs) with proper time-delay between each channel. In the proof-of-concept experiment, due to the unavailable of many MODs, only the odd and even channels are de-multiplexed. They are then modulated by using two Mach-Zehnder modulators (MZMs) with different signals. Then different modulated optical combs are combined to produce the AO-OFDM-SC, which is then transmitted through 40 km single mode fiber (SMF) to the remote antenna unit and optical networking unit (RAU/ONU).

Inset of Fig. 1 shows the schematic optical spectrum of the AO-OFDM-SC for both wired and wireless applications. The AO-OFDM is used for the wired application launching to the AO-OFDM receiver (Rx), while the O-OFDM is used for the wireless application launching to the optical filter (OF) followed by an uni-traveling carrier photodiode (UTC-PD). At the RAU/ONU, the downstream signal is power divided for the wireless and wired applications. For the wireless application, a tunable bandwidth OF or wavelength selective switch (WSS) is used to select the optical two tones, which will be launched to the UTC-PD to generate the MMW signal. The MMW signal is transmitted via a pair of w-band horn antenna. After the wireless transmission, at the mobile device the signal is received, amplified by a low noise amplifier (LNA), and envelope-detected for the bit-error-rate (BER) measurement. In the

proof-of-concept demonstration, the WSS is the liquid-crystal based device (Finisar Waveshaper 4000s), with Gaussian-shaped 3-dB bandwidth of 8 GHz, insertion loss of 5 dB, polarization dependent loss (PDL) of 0.2 dB. Monolithic integrated OF using silicon-based cascaded micro-ring resonators could also be used [11]. In order to provide flexible wireless services, the WSS can select different optical two tones from the downstream signal; hence different MMW frequencies (generated by the coherent-beating of the two tones in the UTC-PD) can be produced to support different wireless cell sizes. For example, the 100 GHz MMW can support very high capacity; however, the wireless transmission distance is short (pico-cell size). When selecting 10 GHz carrier frequency, low capacity is supported; however, the wireless transmission distance is long (macro/micro cell). The feature of flexibly supporting a hierarchy of different cells is desirable for future convergent networks [12].

For the wired application, the AO-OFDM-SC is launched to the AO-OFDM Rx as shown in the RAU/ONU in Fig. 1. In the proof-of-concept demonstration, the de-multiplexer is a 100 ps optical delay interferometer (DI) (Optoplex DPSK Demodulator) with free spectral range (FSR) of 10 GHz, insertion loss of 2.2 dB and PDL of 0.2 dB. It de-multiplexes the odd and even AO-OFDM signal at the two output ports. Then an OF after one output port can select one AO-OFDM sub-channel for BER measurement. In principle, each sub-channel of the AO-OFDM signal can be de-multiplexed simultaneously using a photonic chip [13, 14]. In order to provide flexible wired application, the AO-OFDM Rx in the RAU/ONU can be upgradeable. This means when using a 20-channel AO-OFDM Rx with 20 PDs, 100 Gb/s data rate can be provided to high capacity ONU. When using a 8-channel AO-OFDM Rx with 8 PDs, 40 Gb/s data rate can be provided to low capacity ONU.
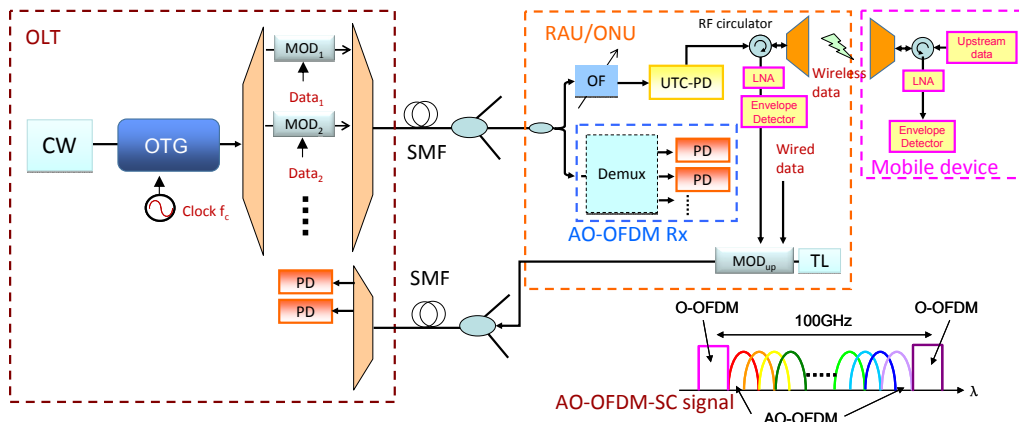

Fig. 1. Architecture of the proposed convergent access network. OTG: optical tone generator, MOD: optical modulator, SMF: single mode fiber, OF: optical filter, PD: photodiode, TL: tunable laser. Inset: schematic optical spectrum of the AO-OFDM-SC.

Figure 1 also includes the conceptual upstream architecture. The upstream MMW signal sending from the mobile device is received, amplified by a LNA, and envelope-detected at the RAU/ONU. A RF circulator connecting the horn antenna can be used to separate the downstream and upstream signals. On the other hand, the wired upstream data will combine with the envelope-detected upstream wireless data to drive the upstream MOD_{up}, which is used to encode the CW signal produced by a tunable laser (TL) to produce the upstream signal.

3. Principle of the AO-OFDM-SC

In this section, we discuss the working principle of the high spectral-efficient AO-OFDM-SC. Figure 2 shows the schematic optical spectra and simulated eye-diagrams (using VPI Transmission Maker V.7.5) for illustrating the operation principle of AO-OFDM, which is also known as coherent-WDM [15]. High spectral-efficiency (channel spacing is equal to the bit-rate). Considering the target wavelength channel at f_0 shown in Fig. 2(a) after passing

through an optical filter (filter pass-band: dotted line), residual crosstalk from the high frequency components of the two adjacent channels will be also inside the pass-band of the optical filter, as shown in Figs. 2(b) and 2(c). The corresponding eye-diagrams are return-to-zero (RZ) liked due to the transient components of the signal in time-domain. By time-aligning these neighbor channel transients to the eye-crossing of the target channel, clear eye-opening can be achieved as shown in Fig. 2(d). Hence, high spectral-efficiency AO-OFDM-SC is obtained, and the data rate of each sub-channel (5 Gb/s) is equal to the sub-channel separation (f_{LO} = 5 GHz) in our experiment.
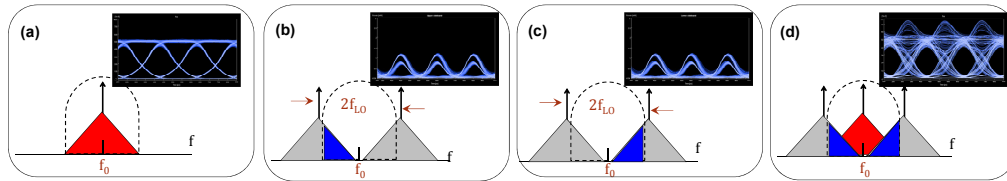

Fig. 2. Schematic optical spectra and simulated eye-diagrams of the AO-OFDM-SC.

4. Experimental results and discussion

We first discuss the MMW wireless application using O-OFDM. Two tones are modulated by an O-OFDM signal via the MODs. The O-OFDM generation is based on off-line Matlab program, including serial-to-parallel conversion, quadrature amplitude modulation (QAM) symbol encoding, and IFFT. The O-OFDM signal has FFT size of 512. It is applied to the MOD via an arbitrary waveform generator (AWG) with 8 GSample/s sampling rate. The bandwidth of the O-OFDM is 4 GHz. In the experiment, the UTC-PD is working at w-band (75-110 GHz), and optical two tones with separation of ~100 GHz are used. To achieve higher data rate, bit-loading is used. The level of bit-loading is determined by the signal-to-noise ratio (SNR). The MMW signal generated by the UTC-PD is transmitted via a pair of w-band horn antenna. The wireless received signal is amplified by a LNA, envelope-detected and captured by a real-time oscilloscope (RTO). The OFDM demodulation process includes off-line synchronization, FFT, one-tap equalization, and QAM symbol decoding. It is also worth to mention that as the O-OFDM is highly spectral-efficient, no spectral overlapping is used for the O-OFDM with the neighbor AO-OFDM sub-channel.
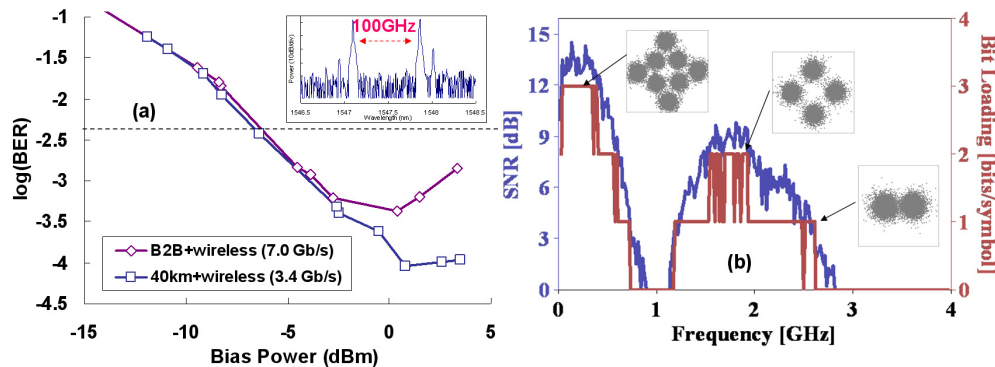

Fig. 3. (a) Measured BER of the O-OFDM MMW signal with both wireless and SMF transmissions. (b) Measured SNR performance of the MMW signal with both wireless and 40 km SMF transmissions.

    Figure 3(a) shows the measured BER performance of the 100 GHz wireless MMW transmission. The MMW signal is generated by selecting 2 optical tones both carrying the same O-OFDM signal. After 40 km SMF transmission, we observe a strong dispersion-induced power fading effect at the received signal. The dispersion-induced power fading

produces the fiber-length and frequency-band dependent power fluctuation at the received signal. This can be observed in the SNR spectrum shown in Fig. 3(b). To achieve higher data rate, bit-loading is used. For higher SNR frequency band, 3 bits/symbol is used, and the maximum data rate after using bit-loading is 3.4 Gb/s. Both measurements satisfy the forward-error-correction (FEC) limit.
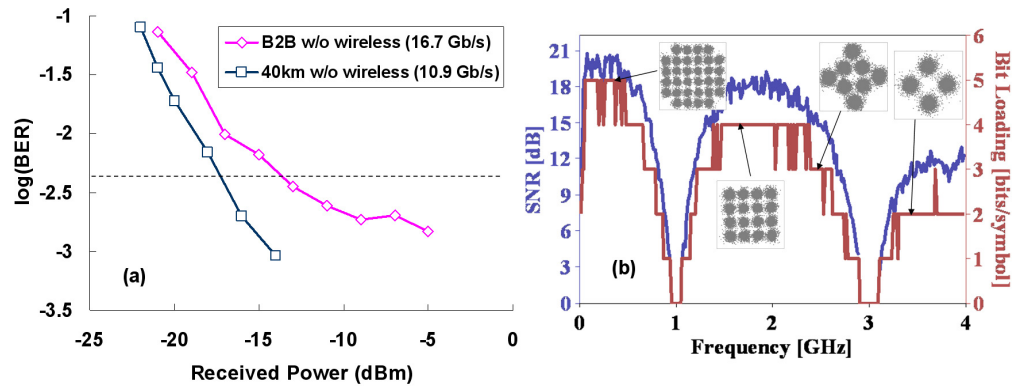

Fig. 4. (a) Measured BER of the O-OFDM MMW signal with SMF transmissions and without wireless transmission. (b) Measured SNR performance of the MMW signal with 40 km SMF transmissions and without wireless transmission.

In order to evaluate the effect of wireless transmission, we then analyze of the MMW ROF transmission without the wireless part. The experimental conditions are the same unless the UTC-PD is replaced by a 10 GHz PIN PD. Figure 4(a) shows the measured BER performance. The maximum data rate achieved is 16.7 Gb/s at back-to-back (B2B), and after 40 km SMF transmission, we still observe the dispersion-induced power fading effect as discussed in last paragraph. Bit-loading is also used to achieve higher data rate as possible, which is shown in Fig. 4(b). For higher SNR frequency band, 5-bit/symbol is used, and the maximum data rate can be significantly increased to 10.9 Gb/s.
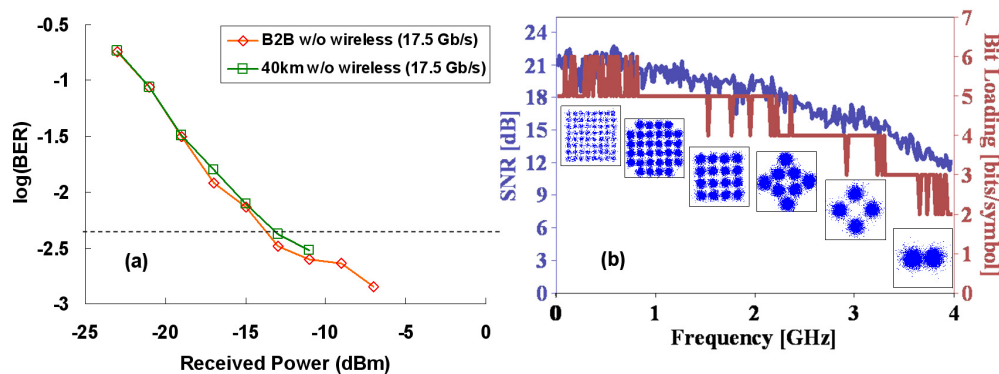

Fig. 5. (a) Measured BER of the O-OFDM MMW signal with power fading mitigation, with SMF transmissions and without wireless transmission. (b) Measured SNR performance of the MMW signal with power fading mitigation, with 40 km SMF transmissions and without wireless transmission.

To mitigate the dispersion-induced power fading effect, only one optical tone carries the O-OFDM signal while the other optical tone which is 100 GHz away is un-modulated. Figure 5(a) shows the BER performance by measuring the baseband OFDM signal. It is observed that there is negligible power penalty within 40 km transmission. Figure 5(b) shows the SNR spectrum, indicating that the power fading effect is mitigated. This increases the available bandwidth and provides a much higher data rate. In this case, 17.5 Gb/s data rate is achieved.

From the experimental results, it is believed that longer transmission distances can be supported. The power fading can also be mitigated using two-chirped-modulator scheme [16]; however, this may increase the system complexity.
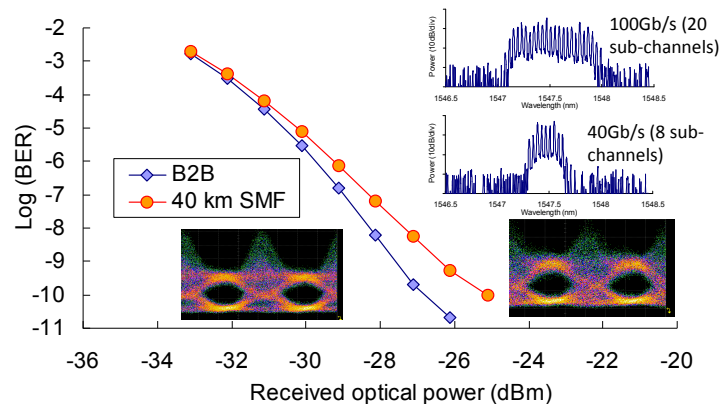

Fig. 6. BER measurements of an AO-OFDM-SC sub-channel. Insets: experimental de-multiplexed eyes at B2B and 40 km SMF; experimental optical spectrum of 100 Gb/s and 40 Gb/s AO-OFDM signals.

Then we discuss the wired application using AO-OFDM. Figure 6 shows the BER measurement of an AO-OFDM-SC sub-channel at B2B and after 40 km SMF de-multiplexed using a DI and OF as described above. About 1-dB power penalty is observed at BER of 10^{-9}. The corresponding NRZ eye-diagrams at B2B and after 40 km SMF are included in Fig. 6. We can observe that the there is a good match of the eye-shape between the experimental result and the simulation result shown in Fig. 2(d). Inset of Fig. 6 shows the optical spectra of 100 Gb/s and 40 Gb/s AO-OFDM signals including 20 sub-channels and 8 sub-channels respectively. From the experimental results, AO-OFDM can be a promising candidate for the future convergent optical wired and wireless access networks as high data rate signal can be easily achieved using all-optically generated orthogonal subcarriers while satisfying the FEC requirement.

4. Conclusion

O-OFDM is a promising candidate for the future high-speed optical access networks. As the O-OFDM signal is electronically generated and demodulated via electronic DAC/ADC, its data rate is limited by the sampling rate of the DAC/ADC. In this work, we proposed and demonstrated the feasibility of using AO-OFDM for the convergent optical wired and wireless access networks. AO-OFDM relies on all-optically generated orthogonal subcarriers; hence, high data rate (> 100 Gb/s) can be easily achieved without hitting the speed limit of electronic DAC/ADC. For the ROF wireless applications, O-OFDM was used. After 40 km SMF transmission, the dispersion-induced power fading effect limited the data rate. The maximum data rate was 3.4 Gb/s. Without the wireless part, the maximum data rate can be increased to 10.9 Gb/s. In order to mitigate the dispersion-induced power fading, only one optical tone carried the O-OFDM signal while the other optical tone was un-modulated. Hence, 17.5 Gb/s data rate was achieved. For the wired application, ~1-dB power penalty was observed at BER of 10^{-9} in an AO-OFDM sub-channel after 40 km SMF transmission.

Acknowledgments